



Chirality dependence of nanoscale ferromagnetic NOT gates

E. R. Lewis, D. Petit, L. O'Brien, H. T. Zeng, D. E. Read et al.

Citation: *J. Appl. Phys.* **109**, 053904 (2011); doi: 10.1063/1.3549599

View online: <http://dx.doi.org/10.1063/1.3549599>

View Table of Contents: <http://jap.aip.org/resource/1/JAPIAU/v109/i5>

Published by the [American Institute of Physics](#).

Related Articles

Temperature-dependent electron transport in highly ordered Co/Al₂O₃ core-shell nanocrystal memory synthesized with di-block co-polymers

J. Appl. Phys. **111**, 064505 (2012)

Spin torque switching of 20nm magnetic tunnel junctions with perpendicular anisotropy

Appl. Phys. Lett. **100**, 132408 (2012)

Ti-electrode effects of NiO based resistive switching memory with Ni insertion layer

Appl. Phys. Lett. **100**, 133502 (2012)

Grain boundaries as preferential sites for resistive switching in the HfO₂ resistive random access memory structures

Appl. Phys. Lett. **100**, 123508 (2012)

Impact of TaO_x nanolayer at the GeSex/W interface on resistive switching memory performance and investigation of Cu nanofilament

J. Appl. Phys. **111**, 063710 (2012)

Additional information on *J. Appl. Phys.*

Journal Homepage: <http://jap.aip.org/>

Journal Information: http://jap.aip.org/about/about_the_journal

Top downloads: http://jap.aip.org/features/most_downloaded

Information for Authors: <http://jap.aip.org/authors>

ADVERTISEMENT



**FIND THE NEEDLE IN THE
HIRING HAYSTACK**

Post jobs and reach
thousands of hard-to-find
scientists with specific skills



<http://careers.physicstoday.org/post.cfm> **physicstoday** JOBS

Chirality dependence of nanoscale ferromagnetic NOT gates

E. R. Lewis,^{1,2,a)} D. Petit,^{1,2} L. O'Brien,^{1,2} H. T. Zeng,¹ D. E. Read,¹ and R. P. Cowburn^{1,2}

¹*Department of Physics, Blackett Laboratory, Imperial College London, London SW7 2BW, United Kingdom*

²*Cavendish Laboratory, University of Cambridge, Cambridge CB3 0HE, United Kingdom*

(Received 12 November 2010; accepted 15 December 2010; published online 9 March 2011)

The behavior of a transverse domain wall (DW) interacting with a ferromagnetic NOT gate is studied with specific emphasis on the role of the DW chirality (sense of rotation of magnetization crossing the DW). We examine both the effect of the incoming DW chirality on the operation of the NOT gate and the effect of the gate on the DW chirality. We find that the chirality of the incoming DW does not affect the range of fields over which the NOT gate operates correctly. The effect of the NOT gate on the DW chirality depends on the chirality of the incoming DW: when the DW is incident on the NOT gate with the wide side of the DW on the inside of the V-shape formed by the gate, the chirality is conserved, but when the DW is incident on the gate with its wide side on the outside of the V-shape, the chirality may reverse. © 2011 American Institute of Physics. [doi:10.1063/1.3549599]

I. INTRODUCTION

The manipulation of domain walls (DWs) in ferromagnetic nanostrips forms the basis of several proposed applications in memory, logic, and sensing. DWs in a nanostrip can be used to store data¹ or propagated through a complex nanostrip network to perform logic operations.² DW-based turn sensors³ and devices for detection or manipulation of functionalized magnetic beads^{4,5} have also been demonstrated. Such devices require control of the DW motion, which in turn may depend on the structure of the DW. In this paper, we study the behavior of ferromagnetic NOT gates,^{6,7} which consist of a cusp-shaped structure (Fig. 1). DWs propagate through the gate under the action of a rotating field with head-to-head and tail-to-tail walls moving on opposite half cycles of the rotating field; the direction of motion is fixed by the sense of rotation of the field and is the same for both head-to-head and tail-to-tail DWs. A NOT gate, or a series of NOT gates, thus provides a mechanism for unidirectional motion of DWs of opposite charge (head-to-head or tail-to-tail) under a global field. The logical NOT operation of the gate consists of reversing the magnetostatic charge of the DW. In this paper, we do not concentrate on the role of the DW charge but instead investigate how the internal structure of the DW affects the operation of a NOT gate. The equilibrium DW structure in thin and narrow nanostrips is a transverse domain wall^{8,9} with an asymmetrical triangular shape, which can be conveniently characterized by the sense of rotation of the magnetization crossing the DW. This is often referred to as the DW handedness or “chirality.”^{10–12} Here we examine the chirality dependence of the NOT gate; we study both the effect of the chirality of the incoming DW on the operation of the gate and the effect of the NOT gate on the chirality of the DW.

II. EFFECT OF DW CHIRALITY ON NOT GATE OPERATION

NOT gates have two distinct failure modes. If the applied field is too large, new domains nucleate whenever the field changes direction, and switching at the output of the gate is observed even when no DW is incident on the gate. If the field is too small, no switching or intermittent switching is observed. The onset of these two failure modes determines the upper (nucleation) and lower (nonswitching) boundaries of the “operating area” (also referred to as the “operating margin”).⁷ The operating area is the area in the H_x – H_y plane for which the NOT gate operates correctly, where H_x and H_y are the semiaxes of the applied elliptical rotating field. In this section, we examine whether the size of the operating area is affected by the chirality of the incoming DW. To provide a DW of known chirality at the input of the gate, we fabricated the structures shown in Fig. 1 using electron beam lithography, thermal deposition of 10 nm of Permalloy ($\text{Ni}_{19}\text{Fe}_{81}$), and a lift-off process. The NOT gates are patterned on nanostrips of width 100 nm with L-shaped [Fig. 1(a)] or C-shaped ends [Fig. 1(b)]. Magnetization switching of the nanostructures was measured using a magneto-optical Kerr effect (MOKE) magnetometer with a focused laser spot diameter of $\sim 5 \mu\text{m}$. The measurement is described in Fig. 2. Figures 2(a) and 2(d) show the applied field sequence and schematics of the magnetization configurations obtained when the NOT gate operates correctly. Figures 2(b) and 2(e) show plots of the applied fields and the Kerr signal measured at the point indicated by the asterisk in Figs. 2(a) and 2(d). The top Kerr trace corresponds to correct operation of the NOT gate, and the lower traces correspond to the two failure modes as described in the following text. Figures 2(c) and 2(f) show the applied fields with H_y plotted as a function of H_x ; the points at which switching occurs for correct operation of the NOT gate are indicated by the filled circles. A saturating field pulse is applied along $(-1, -1)$ [i in Figs. 2(a)–2(c) and 2(d)–2(f)] to create two DWs: one at one

^{a)}Author to whom correspondence should be addressed. Electronic mail: e.lewis06@imperial.ac.uk.

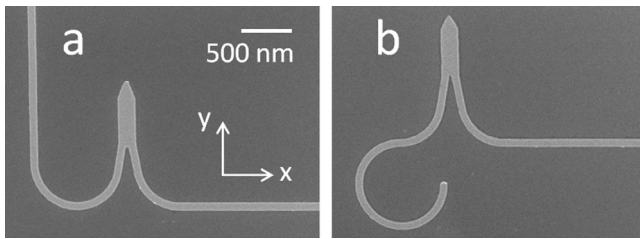


FIG. 1. SEM images of structures used for chirality dependence measurement. (a) Structure with L-shaped end. (b) Structure with C-shaped end. The right-hand part of each structure is a straight nanostrip extending for $9 \mu\text{m}$ past the NOT gate.

corner of the L- or C-shape and one on the right-hand side of the NOT gate. A small field along $+x$ is then applied to expel the right-hand DW [ii in Figs. 2(a)–2(c) and 2(d)–2(f)] and thus switch the magnetization in the right-hand part of the structure. This switching event is detected using the MOKE, producing an upward step in the Kerr signal. In the case of the L-shape, the small field along $+x$ also causes the left-hand DW to move to the left-hand edge of the NOT gate; for the C-shaped structure, an additional field step is necessary [iii in Fig. 2(d)] to bring the left-hand DW around the curve of the C-shape and up to the edge of the NOT gate. We label the configuration as “out” when the wide side of the incoming DW is on the outside of the V-shape formed by the NOT gate [iii in Fig. 2(d)] and “in” when the wide side of the DW

is on the inside of the V-shape [ii in Fig. 2(a)]. Two full cycles of an anticlockwise rotating field are then applied. If the NOT gate is operating correctly, the DW moves through the gate during the first half cycle [ii–iv in Figs. 2(a)–2(c) and iii–v in 2(d)–2(f)], again switching the magnetization in the right-hand part of the structure, and no switching is observed on the subsequent half cycles. This corresponds to the topmost (black) Kerr signal trace in Figs. 2(b) and 2(e). If the rotating field is large enough to cause renucleation, switching is observed on every half cycle of the rotating field, as in the middle (gray) Kerr signal trace. If the rotating field is too small, no switching is observed until the saturating field is reapplied, as in the bottom (gray) Kerr signal trace. These three distinct switching patterns allow us to map out the operating area. Figure 3 shows the operating areas for different DW chiralities in two types of NOT gate. The data do not provide evidence for any dependence on chirality. This is consistent with previous work^{6,7} in which the NOT gate operated correctly as part of a ring oscillator structure; in a ring oscillator, the chirality is not controlled and may reverse as the DW travels several tens of microns around the loop.^{13–15}

Note that chirality reversal might also be expected for the C-shaped structures used here because the DW must travel $\sim 2.5 \mu\text{m}$ around the C-shape before reaching the NOT gate, and the minimum distance for chirality reversal in a straight nanostrip of similar dimensions has been

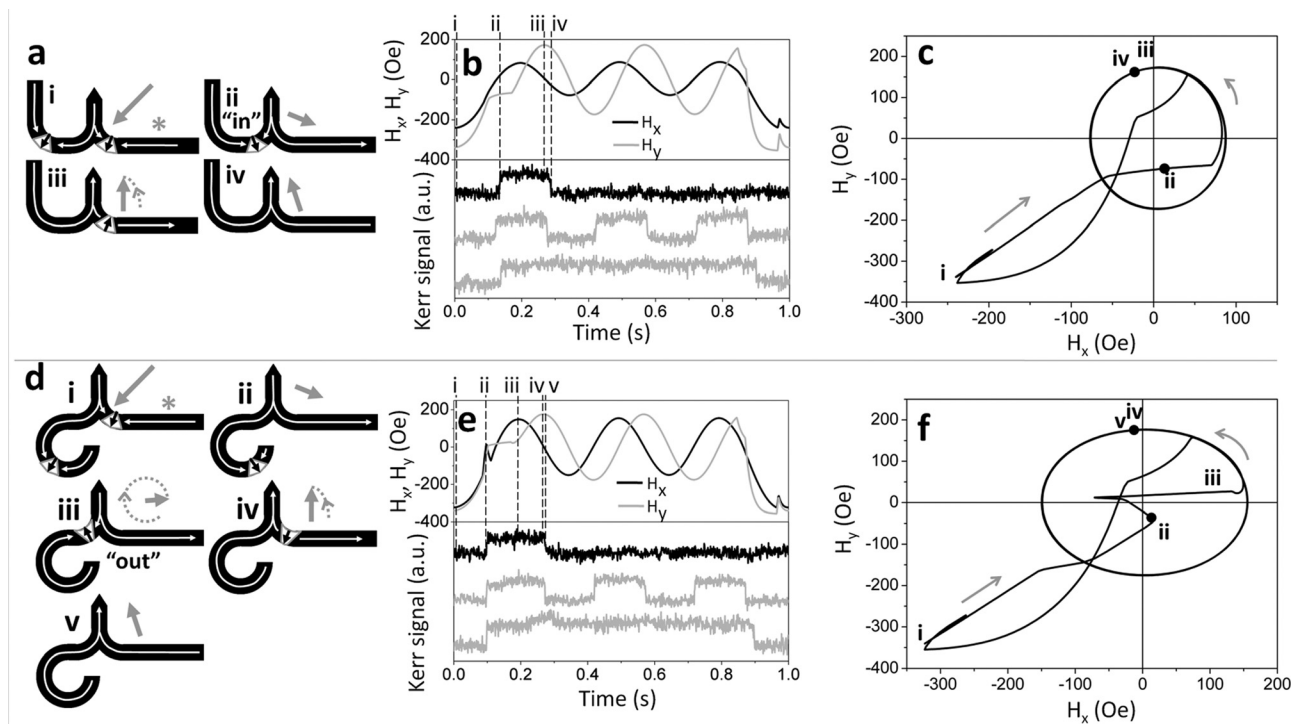


FIG. 2. Testing the chirality dependence of a NOT gate. (a) Schematics showing the applied field sequence and resulting magnetisation configurations for L-shaped structures, where the DW is incident on the gate in the “in” configuration. The position of the MOKE laser spot is indicated by the gray asterisk in (a) i. (b) Plots of H_x and H_y as a function of time (upper panel) and examples of the measured Kerr signal (lower panel). The top trace (black) shows the measured switching pattern when the NOT gate is operating correctly; the middle trace (gray) shows the switching pattern when the magnitude of the elliptical rotating field is too large; and the bottom trace (gray) shows the switching pattern when the rotating field is too small. The dashed lines labeled i–iv correspond to the stages i–iv shown in (a). (c) An alternative way to visualize the applied field and switching pattern. The black line shows H_y as a function of H_x and the black filled circles indicate the points at which switching occurs. The data shown correspond to correct operation of the NOT gate. (d)–(f) Equivalent schematics and plots for C-shape structures, where the DW is incident on the gate in the “out” configuration.

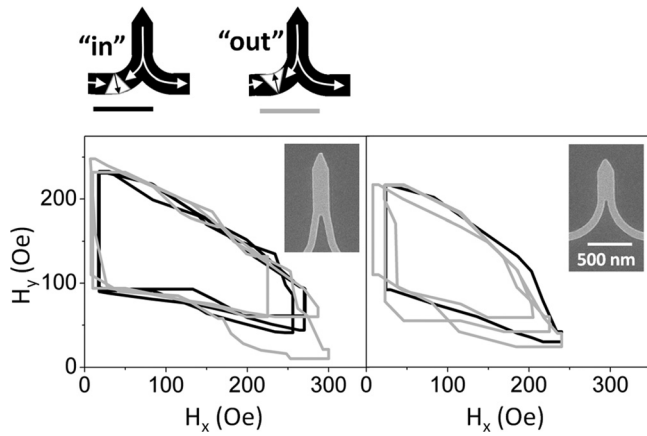


FIG. 3. Operating areas for DWs of different chiralities. The plots show measured operating areas for two types of NOT gate (SEM images in the insets) for DWs incident on the gate in the “in” (black) and “out” (gray) configurations. Each trace corresponds to a separate structure.

measured as $1.6 \pm 0.25 \mu\text{m}$.¹⁶ However, this chirality reversal is a dynamical effect¹⁵ that occurs during continuous motion of the DW. Such a continuous motion is not expected to occur on the C shape because the rate of rotation of the field is slow compared with the domain wall motion: the rate of change of the field is less than 10 kOe s^{-1} , and the minimum DW velocity is around 50 m s^{-1} ,¹⁷ corresponding to a travel time over $3 \mu\text{m}$ of 60 ns . The maximum change in the field during this time is less than 1 mOe . Thus, the magnetization always relaxes to an equilibrium configuration before there is an appreciable change in the field, and the DW is expected to make a series of small steps around the curve of the C-shape. Therefore, it is not expected that chirality reversal should occur as the DW moves toward the NOT gate.

III. EFFECT OF NOT GATES ON DW CHIRALITY: TESTING FOR CHIRALITY CONSERVATION

In the previous section, we looked at the effect of the incoming DW chirality on the operation of the NOT gate; in this section, we examine the effect of the NOT gate on the chirality of the DW. Specifically, we test whether the chirality of the incoming DW is preserved as it passes through the NOT gate. (A head-to-head DW with core magnetization pointing along character has the same chirality as a tail-to-tail DW with core magnetization pointing along $\pm y$.) To test whether the NOT gate is chirality-conserving, the experiment described in the preceding text is extended by adding a chirality-dependent trap at the output of the NOT gate. The chirality of the DW exiting the gate can be detected by measuring the field required to transmit this DW through the trap. We used T-shaped traps, for which the switching fields for DWs of different chiralities are well-separated as described in Ref. 18.

Before testing the NOT gate structures with traps, it is necessary to measure the switching fields for each different DW-trap configuration (without a NOT gate). These measurements were already carried out in Ref. 18, but for nanostraps of different dimensions, which were fabricated

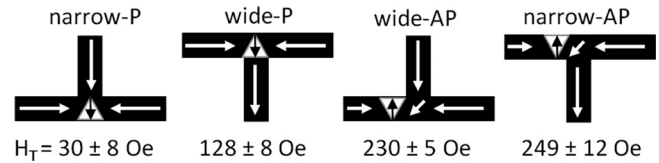


FIG. 4. Switching fields for different DW-trap configurations. The switching fields were measured on five nominally identical structures of each type.

using focused ion beam patterning rather than electron beam lithography. We therefore fabricated additional structures with a trap only (no NOT gate) and measured the transmission field for each different DW-trap configuration. There are four possible configurations, because the magnetization in the core of the DW may be either parallel or antiparallel to the magnetization in the transverse arm of the T-shape, and the transverse arm may be either on the wide or the narrow edge of the DW. The four configurations are labeled wide-P (parallel), wide-AP (antiparallel), narrow-P, and narrow-AP, as illustrated in Fig. 4. The transmission fields (values of H_x at which the DW passes the trap) are lower in the two parallel cases: from measurements on five structures of each type, we obtained values of $30 \pm 8 \text{ Oe}$ (narrow-P) and $128 \pm 8 \text{ Oe}$ (wide-P), whereas in the antiparallel configurations, the switching fields were $249 \pm 12 \text{ Oe}$ (narrow-AP) and $230 \pm 5 \text{ Oe}$ (wide-AP). (These switching fields were measured in the presence of a constant $H_y \sim 10\text{--}20 \text{ Oe}$.) Distinguishing between DWs of opposite chiralities corresponds to distinguishing between parallel and antiparallel switching fields (i.e. distinguishing narrow-P from wide-AP or wide-P from narrow-AP); the clear difference in magnitude between the parallel and antiparallel switching fields means that different chiralities can reliably be distinguished. Note that micromagnetic simulations¹⁸ showed that in the narrow-AP case, the DW incident on the trap splits into two DWs; the second DW moves along the vertical arm and switches it. In the wide-AP case, the “transmission field” does not correspond to transmission of the DW past the trap, but instead to re-nucleation of a new domain next to the trap.¹⁸

Having established the switching fields for each different DW-trap configuration, we can proceed to test

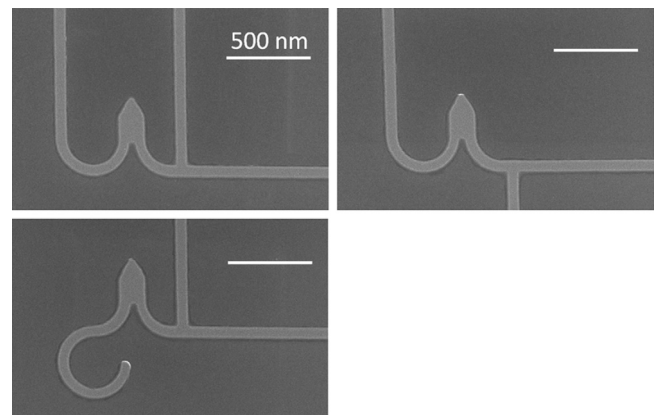


FIG. 5. SEM images of NOT gate structures with traps. The scale is the same for all three images.

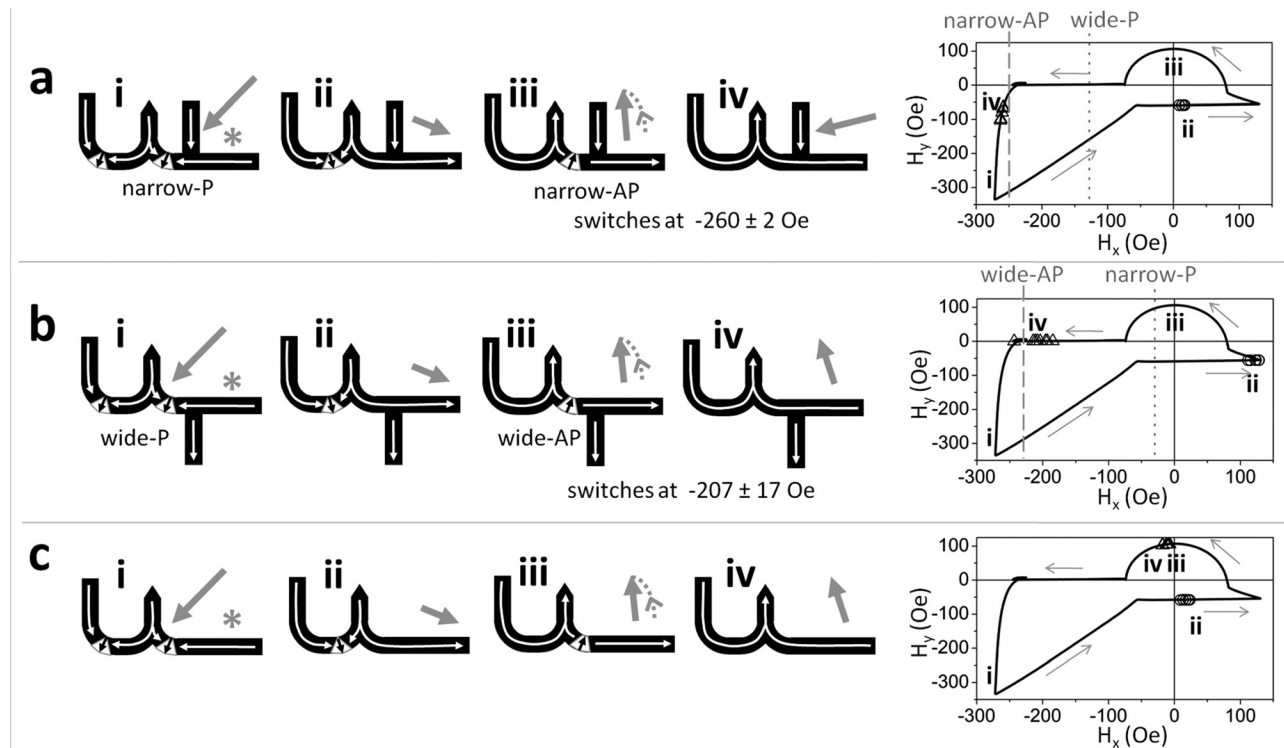


FIG. 6. Testing for chirality conservation when the DW is incident on the gate in the “in” configuration. The schematics show the applied field sequence and resulting magnetisation configurations, assuming chirality conservation. The position of the MOKE laser spot is indicated by the asterisk. The experimental results are displayed on the plots at right. The dashed and dotted lines indicate the switching fields for the two possible DW-trap configurations (see Fig. 4): the dashed line indicates the expected switching field if the chirality is conserved, and the dotted line indicates the expected switching field if the chirality reverses. The black line shows H_y as a function of H_x , and the first and second switching events occur at the points marked by the circles and triangles, respectively. Each circle+triangle pair corresponds to a separate structure; 9 or 10 structures of each type were measured. The roman numerals on the plots indicate the corresponding schematic. For both trap positions (a), (b), the second transition (triangles) always occurs in an antiparallel configuration and corresponds to chirality conservation.

chirality conservation in the NOT gate. We performed the experiment with both chiralities of DW at the input of the NOT gate. Figure 5 shows scanning electron microscope (SEM) images of the NOT gate structures with traps. Figure

6 illustrates the measurement for the “in” configuration (L-shaped structures). The MOKE laser spot is positioned on the right-hand part of the structure, as indicated by the asterisks in Fig. 6. The schematics show the applied field

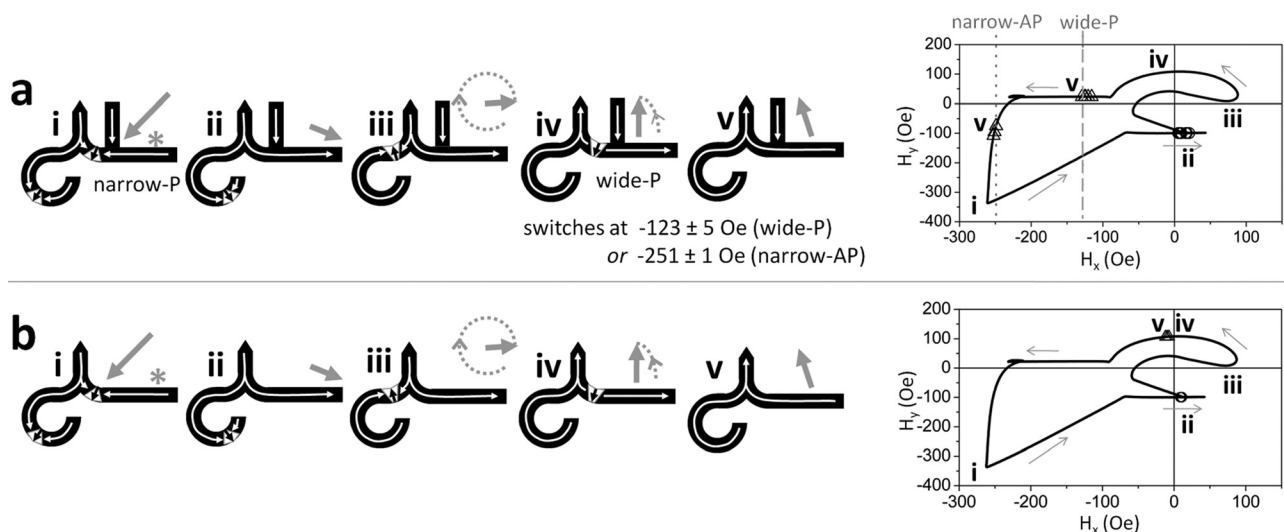


FIG. 7. Testing for chirality conservation when the DW is incident on the gate in the “out” configuration. The schematics show the applied field sequence and resulting magnetization configurations assuming chirality conservation, and the experimental results are displayed on the plots at right. The position of the MOKE laser spot is indicated by the asterisk. The dashed and dotted lines on the plot indicate the switching fields for the two possible DW-trap configurations (see Fig. 4): the dashed line indicates the expected switching field if the chirality is conserved, and the dotted line indicates the expected switching field if the chirality reverses. The symbol assignments are as in Fig. 6. When the trap is present (a), the second transition (triangles) may occur at two different fields, showing that the chirality is not always conserved.

sequence and resulting magnetization configurations in the case where the chirality of the DW is conserved. The experimental results are shown on the graphs, which illustrate the switching behavior of the structures: the black line shows H_y as a function of H_x , and the fields at which the first and second switching events occur are indicated by the circles and triangles, respectively, where each circle–triangle pair corresponds to a separate structure. The arrows indicate the trajectory in the H_x – H_y plane, and the roman numerals indicate the corresponding schematic. The dashed lines on the plots indicate the switching fields for the two possible DW–trap configurations when the second DW exits the NOT gate as given on Fig. 4. The measurement was performed with the trap on the upper side of the nanostrip [Fig. 6(a)], with the trap on the lower side of the nanostrip [Fig. 6(b)], and without any trap [Fig. 6(c)]. When the trap is on the upper side of the nanostrip [Fig. 6(a)], the first DW is in the narrow-P configuration and passes the trap at $H_x = 13 \pm 3$ Oe, $H_y = -58$ Oe; if the chirality is conserved, the second DW will reach the trap in the narrow-AP configuration for which the switching field is ~ 250 Oe, whereas if the chirality reverses, the DW will reach the trap in the wide-P configuration for which the switching field is ~ 130 Oe (Fig. 4). As shown on the H_y vs. H_x plot, all 10 of the measured structures show a second transition at $H_x = -260 \pm 2$ Oe, $H_y = -80 \pm 16$ Oe, which is consistent with chirality conservation. When the trap is on the lower edge of the nanostrip [Fig. 6(b)], the first DW is in the wide-P configuration and passes the trap at $H_x = 119 \pm 6$ Oe, $H_y = -56$ Oe, whereas the second will be in the wide-AP configuration (switching field ~ 230 Oe) if the chirality is conserved and the narrow-P configuration (switching field ~ 30 Oe) if it is not. Again, the experimental data are consistent with chirality conservation because the second transition occurs at $H_x = -207 \pm 17$ Oe, corresponding to the wide-AP configuration. Finally, the bottom panel [Fig. 6(c)] shows the results when the same field sequence is applied to a NOT gate with no trap; the transitions occur at $H_x = 17 \pm 4$ Oe, $H_y = -58$ Oe and $H_x = -12 \pm 4$ Oe, $H_y = 105 \pm 1$ Oe. These fields are comparable to those plotted in Fig. 2(c) and indicate that the NOT gate is operating correctly on application of this field sequence.

For the C-shape structures, only two types of measurement were performed: one with the trap on the upper edge of the nanostrip and one with no trap. The measurements are illustrated in Fig. 7. Figure 7(a) shows the measurement with the trap. In this case, the first DW is in the narrow-P configuration and passes the trap at $H_x = 10 \pm 5$ Oe, $H_y = -99$ Oe. If the chirality is conserved, the second DW will reach the trap in the wide-P configuration and pass the trap at ~ 130 Oe; if the chirality reverses, the DW will reach the trap in the narrow-AP configuration and pass the trap at ~ 250 Oe. The plot in Fig. 7(a) shows that both switching patterns are observed: 6 of the 10 measured structures have a second transition (corresponding to the second DW exiting the NOT gate and passing the trap) at $(H_x = -123 \pm 5, H_y = 23)$ Oe, consistent with chirality conservation, but the remaining four structures have a second transition at $(H_x = -251 \pm 1, H_y = -43 \pm 14)$ Oe, corresponding to chirality reversal. This

higher switching field is close to that shown in Fig. 6(a), which is consistent with the DW being in the narrow-AP configuration in both cases. The DW chirality must therefore have changed at some point after its initial creation: before it reaches the NOT gate, during the transmission through the NOT gate, or in moving from the NOT gate to the trap. As described in the previous section, it is not expected that the DW chirality should reverse as it travels around the curved section of the nanostrip preceding the NOT gate. In addition, measurements on structures with a trap only did not show any evidence of this behavior. One other possibility is that the transverse arm itself might switch. However, we tested this by repeating the measurement of Fig. 7 but with both the applied field and the sample rotated through 90° , so that the Kerr effect measurement was sensitive to the magnetization direction in the transverse arm. No switching was observed on the five structures measured. The results of these tests suggest that it is the interaction with the NOT gate itself that gives rise to chirality reversal in some cases in the “out” configuration. The fact that nominally identical structures in the “out” configuration behave differently from each other suggests that the switching process in this case depends sensitively on small structural imperfections or small variations in the applied field. Note that micromagnetic simulations of an alternative NOT gate design¹⁹ showed different switching mechanisms in the “in” and “out” cases but with chirality conservation observed in both cases.

IV. CONCLUSIONS

In this paper, we have studied the chirality dependence of a ferromagnetic NOT gate. We examined both the effect of the DW chirality on the NOT gate operating area (the range of fields for which the gate operates correctly) and the effect of the gate on the DW chirality. We do not see evidence of any chirality dependence of the operating area. The effect of the NOT gate on the DW chirality appears to depend on the chirality of the incoming DW: when the DW is incident on the NOT gate with the wide side of the DW on the inside of the V-shape formed by the gate, the chirality is conserved, but when the DW is incident on the gate with its wide side on the outside of the V-shape, the chirality may reverse.

ACKNOWLEDGMENTS

The work and results reported in this letter were obtained with research funding from the European Community under the Seventh Framework Programme Contract No. 247368: 3SPIN.

¹S. S. P. Parkin, M. Hayashi, and L. Thomas, *Science* **320**, 190 (2008).

²D. A. Allwood, G. Xiong, C. C. Faulkner, D. Atkinson, D. Petit, and R. P. Cowburn, *Science* **309**, 1688 (2005).

³M. Diegel, S. Glathe, R. Mattheis, M. Scherzinger, and E. Halder, *IEEE Trans. Magn.* **45**, 3792 (2009).

⁴M. Donolato, P. Vavassori, M. Gobbi, M. Deryabina, M. F. Hansen, V. Metlushko, B. Ilic, M. Cantoni, D. Petti, S. Brivio, and R. Bertacco, *Adv. Mater.* **22**, 2706 (2010).

⁵P. Vavassori, V. Metlushko, B. Ilic, M. Gobbi, M. Donolato, M. Cantoni, and R. Bertacco, *Appl. Phys. Lett.* **93**, 203502 (2008).

- ⁶D. A. Allwood, G. Xiong, M. D. Cooke, C. C. Faulkner, D. Atkinson, N. Vernier, and R. P. Cowburn, *Science* **296**, 2003 (2002).
- ⁷D. A. Allwood, G. Xiong, M. D. Cooke, C. C. Faulkner, D. Atkinson, and R. P. Cowburn, *J. Appl. Phys.* **95**, 8264 (2004).
- ⁸R. D. McMichael and M. J. Donahue, *IEEE Trans. Magn.* **33**, 4167 (1997).
- ⁹Y. Nakatani, A. Thiaville, and J. Miltat, *J. Magn. Magn. Mater.* **290**, 750 (2005).
- ¹⁰M. Hayashi, L. Thomas, C. Rettner, R. Moriya, X. Jiang, and S. S. P. Parkin, *Phys. Rev. Lett.* **97**, 207205 (2006).
- ¹¹L. K. Bogart, D. Atkinson, K. O'Shea, D. McGrouther, and S. McVitie, *Phys. Rev. B* **79**, 054414 (2009).
- ¹²S. M. Seo, K. J. Lee, S. W. Jung, and H. W. Lee, *Appl. Phys. Lett.* **97**, 032507 (2010).
- ¹³M. Hayashi, L. Thomas, C. Rettner, R. Moriya, and S. S. P. Parkin, *Nat. Phys.* **3**, 21 (2007).
- ¹⁴Y. Nakatani, A. Thiaville, and J. Miltat, *Nat. Mater.* **2**, 521 (2003).
- ¹⁵A. Thiaville and Y. Nakatani, *Spin Dynamics in Confined Magnetic Structures III*. (Springer-Verlag, Berlin, Germany, 2006).
- ¹⁶E. R. Lewis, D. Petit, A.-V. Jausovec, L. O'Brien, D. E. Read, H. T. Zeng, and R. P. Cowburn, *Phys. Rev. Lett.* **102**, 057209 (2009).
- ¹⁷E. R. Lewis, D. Petit, L. O'Brien, A. Fernandez-Pacheco, J. Sampaio, A.-V. Jausovec, H. T. Zeng, D. E. Read, and R. P. Cowburn, *Nat. Mater.* **9**, 980 (2010).
- ¹⁸D. Petit, A.-V. Jausovec, H. T. Zeng, E. Lewis, L. O'Brien, D. Read, and R. P. Cowburn, *Phys. Rev. B* **79**, 214405 (2009).
- ¹⁹H. T. Zeng, D. Read, L. O'Brien, J. Sampaio, E. R. Lewis, D. Petit, and R. P. Cowburn, *Appl. Phys. Lett.* **96**, 262510 (2010).